Dipole approximation in electron-energy-loss spectroscopy: K-shell excitations

D. K. Saldin and J. M. Yao
Department of Physics and Laboratory for Surface Studies, University of Wisconsin-Milwaukee, P.O. Box 413, Milwaukee, Wisconsin 53201
(Received 16 May 1989)

We investigate the conditions for the validity of the "dipole approximation" in electron-energy-loss spectroscopy (EELS) of atomic K-shell excitations on an analytic model that takes account of the wave function of the ejected core electron, as well as that of the core state. We derive, for the first time, a closed-form expression for the limiting magnitude q_d of the momentum-transfer vector, as a function of both the atomic number and the energy ε of the ejected core electrons. We find that the value currently assumed, namely $q_d = Z^*$, where Z^* is the effective nuclear charge, is only strictly valid in the limit of low energies of the ejected core electron. In fact q_d decreases noticeably with increasing ε. Matrix elements with many different values of q contribute to a typical EELS signal, but the dominant ones lie close to the minimum value $q_{\min}$. The increase of $q_{\min}$ with ε coupled with the decrease of q_d with the same quantity makes it easier to satisfy the conditions for the dipole approximation in the near edge rather than the extended-fine-structure region of the energy-loss spectrum. Our analytic approach is well suited for extension to the cases of other absorption edges (e.g., L, M, edges, etc.).

I. INTRODUCTION

A plot of the inelastic-scattering cross section for a beam of electrons of sufficiently high energy versus energy contains sawtooth-shaped edges for magnitudes of energy loss corresponding to the minima for the excitation of atomic core electrons.[1] These structures are similar to the absorption edges observed when the energies of incident x-ray photons are continuously tuned through atomic core-electron binding energies.[2] If the atoms concerned are in the near vicinity of other atoms, as in the case of a sample of condensed matter, fine structures are observed on both forms of absorption edges[3,4] which are characteristic of the nature and disposition of the surrounding atomic environment. The relatively prominent features within a few tens of electron volts (eV's) of the absorption edges are termed the x-ray-absorption near-edge structure (XANES) (Ref. 5) in the x-ray case, and electron-energy-loss near-edge structure (ELNES) (Ref. 6) in the case of the electrons. These structures are determined by the quite strong multiple scattering from nearby atoms, of core electrons ejected with relatively low energies. Beyond a few tens of eV's and extending up to several hundred eV's are to be found the so-called extended x-ray and electron-energy-loss fine structures, EXAFS's (Refs. 3, 7, and 8) and EXELFS's (Ref. 9) respectively, determined by weaker backscattering events of ejected core electrons of higher energies.

Experimentally measured near-edge and extended fine structures are frequently remarkably similar for the two forms of incident radiation. It is well known that in the limit of small momentum transfer in an electron energy-loss process, the matrix element for the inelastic-scattering event reduces to one of essentially the same form as that for x-ray absorption, namely an electric-dipole (or "optical") matrix element. Matrix elements of this reduced form are said to employ the "dipole approximation."[4] In this limit, electric-dipole selection rules relate the angular-momentum quantum numbers of the core and ejected electrons. On the other hand, under certain conditions, "nondipole" effects, signaling the breakdown of this approximation, have been observed.[10,11] The interpretation of electron-energy-loss experiments would be considerably simplified if the dipole approximation could be used. Clearly therefore, it would be helpful to formulate some rules for determining the conditions under which that approximation may be confidently assumed. The conventional derivation of these rules considers only the fact that the core wave function acts as an envelope on the integrand of the radial matrix element for the atomic transition. As shown in Sec. III A, this leads to the simple condition

$$q \ll q_d \ , \tag{1}$$

where

$$q_d = \frac{1}{r_c} \tag{2}$$

for the validity of the dipole approximation core-excitation EELS. In the preceding expressions q is the magnitude of the momentum-transfer vector, q_d its limiting value, and r_c the radial extent of the core wave function. For K-shell electrons, $r_c \simeq 1/Z^*$ (in atomic units), where Z^* is the effective nuclear charge, and

$$q_d \simeq Z^* \ . \tag{3}$$

However, the excited-state wave function, which also forms part of the integrand, is a quantity which depends on the energy ϵ of the ejected core electron, and could

conceivably affect the value of this limit. There have been some indications of this in numerical investigations of the relative magnitudes of the matrix elements coupling the core states to different angular-momentum-resolved excited states, for different values of q and ϵ,[12] but a systematic investigation of the variation of q_d for a wide range of values of ϵ across the Periodic Table of elements has not been attempted. This is not surprising in view of the extensive numerical labor involved in such an approach, since both the initial core and excited electron states are found by radial integration of the Schrödinger equation, the matrix element evaluated by numerical integration afterwards, and the computations repeated for points on a *three*-dimensional parameter space representing arbitrary variations of Z, q, and ϵ.

We show in this paper that this question may be investigated much more directly and effectively on the basis of a "hydrogenic" model, similar to one used to calculate generalized oscillator strengths for such atomic transitions.[13,14] The results may be expressed as a partition of the three-dimensional parameter space into a region where the dipole approximation is valid and one in which it may not be assumed, and the surface separating these regions may be determined. We find that the simple result (3) is the asymptotic limit for small ϵ, but that as ϵ is increased, q_d falls noticeably below this value. The consequences of this result for the design of an experiment to ensure the validity of analyses of the results, based on the assumption of the dipole approximation, are discussed. Our method may be extended to cover other absorption edges (e.g., L,M edges, etc.).

II. THEORETICAL BACKGROUND

The general theory of electron-energy-loss spectroscopy (EELS), where an electron is incident on a sample of condensed matter, excites an atomic core electron, and suffers energy loss as a result, can be considerably more complicated than the corresponding theories for x-ray absorption. Firstly, electrons scatter from atoms much more strongly than x rays and the multiple scattering of the incident and detected electrons generally needs to be evaluated.[15–20] Secondly, quantum indistinguishability requires the probability of an energy-loss process taking place to be evaluated by summing the amplitudes of both direct and exchange processes.[18,19] Thirdly is the effect which will be the primary concern of this paper, namely the "nondipole" nature of the excitation matrix elements.

Of course, under many circumstances in EELS all these effects are closely interrelated, and a full theory is very complicated and certainly requires numerical treatment at present. However, in order to achieve an understanding of each effect it is necessary first to study them in isolation.

In order to study the properties of the excitation matrix elements, it is helpful to consider a situation in which the multiple scattering of the projectile electrons is minimized. This can be achieved in transmission EELS experiments, usually induced by high-energy ($\sim$100 keV) electrons in an electron microscope, by using a thin film as a sample, and if it were crystalline, by tilting the sample so that no strong Bragg reflection were excited (cf. the weak-beam method in electron microscopy,[21] which can be successfully analyzed by a kinematic theory). In reflection EELS such conditions may be approached in a material with no long-range order. In such a case, an incident electron beam would generate only diffuse elastic scattering[22] and not Bragg beams (except in the special case of quasicrystals).

In high-energy transmission EELS, exchange effects play no significant role, and they may not contribute much to the measured signals, even in typical lower-energy reflection EELS experiments. However, following the treatment of exchange effects of Ochkur[23] and Saldin,[20] retaining terms due to this effect poses no great further complications, and we do so in our theory. Throughout the development of the theory, we use Hartree atomic units (where Planck's constant $\hbar$ the charge e, and mass m of the electron are taken to be of unit magnitude). In the discussion at the end of this paper, however, we relate our results to units perhaps more familiar to experimentalists, like electron volts (eV's) and ångstroms (Å).

Under such conditions, we may regard the incident beam as a plane wave of energy E_i, say

$$\psi_i(\mathbf{r})=\frac{1}{L^{3/2}}\exp(i\mathbf{k}_i\cdot\mathbf{r}) , \tag{4}$$

where $\mathbf{k}_i$ is its wave vector, L the linear dimension of our apparatus, and $\mathbf{r}$ a position vector. Similarly, an electron detected by a small-angle energy analyzer can represented by

$$\psi_f(\mathbf{r})=\frac{1}{L^{3/2}}\exp(i\mathbf{k}_f\cdot\mathbf{r}) , \tag{5}$$

a plane wave of wave vector $\mathbf{k}_f$ and energy E_f. If the wave function of the core electrons were $\Phi_c(\mathbf{r})$ of energy E_c and that of the excited state $\Phi_x(\mathbf{r})$ of energy ϵ, the double-differential cross section for the process can be written

$$\frac{\partial^2\sigma}{\partial E_f\partial\Omega}=\frac{1}{4\pi^2}\frac{k_s}{k_i}\sum_f |M|^2\delta(E_i+E_c-E_f-\epsilon) , \tag{6}$$

where Ω is a scattering solid angle and

$$M=M_1+M_2 , \tag{7}$$

where

$$M_1=\int \psi_f^*(\mathbf{r})\Phi_x^*(\mathbf{r}')\frac{1}{|\mathbf{r}-\mathbf{r}'|}\Phi_c(\mathbf{r}')\psi_i(\mathbf{r})d\mathbf{r}\,d\mathbf{r}' , \tag{8}$$

$$M_2=\int \Phi_x^*(\mathbf{r})\psi_f^*(\mathbf{r}')\frac{1}{|\mathbf{r}-\mathbf{r}'|}\Phi_c(\mathbf{r}')\psi_i(\mathbf{r})d\mathbf{r}\,d\mathbf{r}' . \tag{9}$$

It is the presence of both these terms M_1 and M_2 which gives rise to the exchange effects in the excitation process. Substituting (4) and (5) in (8) and (9), and assuming $\Phi_c(\mathbf{r})$ varies slowly compared to $\exp(i\mathbf{k}_f\cdot\mathbf{r})$ so that use may be made of the asymptotic expansion

$$\int \Phi(\mathbf{r}')\frac{\exp(i\mathbf{k}_f\cdot\mathbf{r}')}{|\mathbf{r}-\mathbf{r}'|}d\mathbf{r}'=\frac{4\pi}{k_f^2}\exp(i\mathbf{k}_f\cdot\mathbf{r})\Phi(\mathbf{r})+O(k^{-3}) , \tag{10}$$

we find, following Ochkur[20] that

$$M(\mathbf{q})=4\pi\left[\frac{1}{q^2}\pm\frac{1}{k_f^2}\right]\int\Phi_x^*(\mathbf{r})\exp(i\mathbf{q}\cdot\mathbf{r})\Phi_c(\mathbf{r})d\mathbf{r} , \tag{11}$$

where

$$\mathbf{q}=\mathbf{k}_i-\mathbf{k}_f . \tag{12}$$

Writing

$$\Delta(\mathbf{r})\equiv 4\pi\left[\frac{1}{q^2}\pm\frac{1}{k_f^2}\right]\exp(i\mathbf{q}\cdot\mathbf{r}) \tag{13}$$

we can express (6) in its alternative form

$$\frac{\partial^2\sigma}{\partial E_f\partial\Omega}=-\frac{1}{4\pi^3}\frac{k_s}{k_i}\int\Phi_c^*(\mathbf{r})\Delta(\mathbf{r})\mathrm{Im}G^+(\mathbf{r},\mathbf{r}',\epsilon)\times\Delta^\dagger(\mathbf{r}')\Phi(\mathbf{r}')d\mathbf{r}\,d\mathbf{r}' , \tag{14}$$

where $G^+(\mathbf{r},\mathbf{r}',\epsilon)$ is the retarded Green function of the excited electron of energy ϵ. The high degree of localization near the atomic nucleus of a deep core state ensures that we need only the form of G^+ near the center of the atom. In this region the atomic potential is effectively spherical, and we may take the angular-momentum representation of $\mathrm{Im}G^+$ in a muffin-tin approximation:[5]

$$\mathrm{Im}G^+(\mathbf{r},\mathbf{r}',\epsilon)=k\sum_{L'L''}R_{l'}(r,\epsilon)Y_{L'}(\hat{\mathbf{r}})\frac{\mathrm{Im}(\tau_{L'L''})}{\sin\delta_{l'}\sin\delta_{l''}}\times Y_{L''}^*(\hat{\mathbf{r}}')R_{l''}(r',\epsilon) , \tag{15}$$

where $R_l(r,\epsilon)$ is the solution of the radial Schrödinger equation within the muffin-tin sphere for an energy ϵ, and matching on to the function $j_l(kr)\cos\delta_l-n_l(kr)\sin\delta_l$ at the muffin-tin radius, where j_l and n_l are spherical Bessel and Hankel functions, respectively, $Y_L(\hat{\mathbf{r}})$ is a spherical harmonic for angular-momentum quantum numbers $(lm)\equiv L$ (say), $\tau_{L'L''}$ are the elements of the site-diagonal scattering path operator[24] for the atom in question, δ_l its phase shift, and $k=\sqrt{2\epsilon}$, the wave number of ejected core electrons in the interstitial region between muffin tins.

If now we represent the core state as the eigenstate

$$\Phi_c(\mathbf{r})\equiv\phi_{nl}(r)Y_L(\hat{\mathbf{r}}) , \tag{16}$$

and making use of (12), (11) may be written

$$\frac{\partial^2\sigma}{\partial E_f\partial\Omega}=-\frac{1}{4\pi^3}\frac{k_s}{k_i}k\sum_{L'L''}T(L,L')\frac{\mathrm{Im}(\tau_{L'L''})}{\sin\delta_{l'}\sin\delta_{l''}}T^*(L'',L) , \tag{17}$$

where

$$T(L,L')\equiv\int\phi_{nl}^*(r)Y_L(\hat{\mathbf{r}})\Delta(\mathbf{r})R_{l'}(r,\epsilon)Y_{L'}(\hat{\mathbf{r}})d\mathbf{r} . \tag{18}$$

Note that apart from the constants outside the summations, (17) and (18) are identical to the expression for the x-ray absorption rate[5] if the perturbation operator $\Delta(\mathbf{r})$ is replaced by

$$i\,\mathbf{A}\cdot\nabla , \tag{19}$$

where $\mathbf{A}$ is the magnetic vector potential.

Further simplication of (17) may be effected by writing

$$\tau=i\mathbf{t}(1-\mathbf{St})^{-1} , \tag{20}$$

where $\mathbf{t}$ is the diagonal atomic t matrix whose elements are given by

$$t_{l'l''}=i\sin\delta_{l'}e^{i\delta_{l'}}\delta_{L'L''} \tag{21}$$

and $\mathbf{S}$ is the reflection matrix[5] of the cluster of nearby atoms surrounding the exciting atom. Of course it is $\mathbf{S}$ which is responsible for the electron-energy-loss near-edge structure (ELNES) and extended electron-energy-loss fine structures (EXELFS's) around absorption edges for core excitation. However, since our main concern in this paper is to examine the behavior of the matrix elements $T(L,L')$, we notice that since the elements of $\mathbf{S}$ are generally small (ELNES and EXELFS are both studies of the *fine* structure around absorption edges) we may make the approximation

$$\tau=i\mathbf{t} , \tag{22}$$

and with (21) and (22), (17) can be written

$$\frac{\partial^2\sigma}{\partial E_f\partial\Omega}\simeq\frac{1}{4\pi^3}\frac{k_s}{k_i}k\sum_{L'}|T(L,L')|^2 . \tag{23}$$

With (13) and (18), making use of the expansion

$$\exp(i\mathbf{q}\cdot\mathbf{r})\equiv\sum_{lm}4\pi i^l j_l(qr)(-1)^m Y_{l-m}(\hat{\mathbf{r}})Y_{lm}(\hat{\mathbf{q}}) \tag{24}$$

and averaging over initial core states of azimuthal quantum number m, Eq. (23) can be written

$$\frac{\partial^2\sigma}{\partial E_f\partial\Omega}=\frac{1}{\pi^2}\frac{k_f}{k_i}k\left[\frac{1}{q^2}\pm\frac{1}{k_f^2}\right]^2\sum_{l'}(2l'+1)\sum_{l''}(2l''+1)[F_{nl,\epsilon l'}^{l''}(q)]^2\left[\begin{bmatrix} l & l'' & l' \\ 0 & 0 & 0\end{bmatrix}\right]^2 , \tag{25}$$

where

$$F_{nl,\epsilon l'}^{l''}(q)=\int_0^\infty\phi_{nl}(r)j_{l''}(qr)R_{l'}(\epsilon,r)r^2dr \tag{26}$$

and

$$\begin{bmatrix} l & l'' & l' \\ 0 & 0 & 0 \end{bmatrix}$$

is a Wigner $3j$ symbol.[25]

III. LIMITS OF THE DIPOLE APPROXIMATION FOR K-SHELL EXCITATIONS

A. Conventional treatment

For K-shell excitations, $n=1$, $l=0$, and nonzero elements of the $3j$ symbols exist only if $l'=l''$. This leads to further simplification of (25), which can be written

$$\frac{\partial^2\sigma}{\partial E_f \partial\Omega}=\frac{1}{\pi^2}\frac{k_f}{k_i}k\left[\frac{1}{q^2}\pm\frac{1}{k_f^2}\right]^2\sum_{l'}(2l'+1)[F^{l'}_{10,\epsilon l'}(q)]^2 \tag{27}$$

on evaluating the $3j$ symbols by the formula[25]

$$\left[\begin{bmatrix} l_1 & l_2 & l_3 \\ 0 & 0 & 0 \end{bmatrix}\right]^2=\frac{(l_1+l_2-l_3)!(l_1+l_3-l_2)!(l_2+l_3-l_1)!}{(l_1+l_2+l_3+1)!}\left[\frac{p!}{(p-l_1)!(p-l_2)!(p-l_3)!}\right]^2, \tag{28}$$

where

$$p=\tfrac{1}{2}(l_1+l_2+l_3)\ . \tag{29}$$

We can understand some aspects of the behavior of the matrix elements,

$$F^{l'}_{10,\epsilon l'}(q)=\int_0^\infty \phi_{10}(r)j_{l'}(qr)R_{l'}(\epsilon,r)r^2dr \tag{30}$$

by noting that the Bessel functions in the leading terms of the summation (24) may be expanded in the following power series:

$$j_0(qr)=1-\frac{(qr)^2}{6}+O((qr)^4)\ , \tag{31}$$

$$j_1(qr)=\frac{(qr)}{3}-\frac{(qr)^3}{30}+O((qr)^5)\ , \tag{32}$$

$$j_2(qr)=\frac{(qr)^2}{15}+O((qr)^4)\ , \tag{33}$$

$$j_3(qr)=O((qr)^3)\ , \tag{34}$$

$$\vdots$$

On a Bohr model $1s$ wave functions ϕ_{10} in (30) are localized to within a radius $\simeq r_c$ of the nucleus, where

$$r_c=\frac{1}{Z}\ . \tag{35}$$

Therefore, if

$$qr_c\ll 1\ , \tag{36}$$

we would expect the matrix elements (30) to be well approximated by the leading terms in the Bessel function expansions (31)–(34). The term in the lowest power of (qr), i.e., $(qr)^0$, is associated with the $F^0_{10,\epsilon 0}$ matrix element in (27), but this term is zero, since it involves the overlap of core and excited-state eigenfunctions of the same Schrödinger equation. The lowest power of (qr) which gives rise to a nonvanishing term in (27) is that in $(qr)^1$ associated with the $F^1_{10,\epsilon 1}$ matrix element. But, (35) and (36) imply that provided

$$q\ll q_d\ , \tag{37}$$

where

$$q_d=Z\ , \tag{38}$$

the term in $l'=1$ will dominate the summation in (27), and the electric-dipole selection rule

$$\Delta l=\pm 1 \tag{39}$$

can be assumed to relate the core and ejected electron states. Thus we begin to see how under some circumstances EELS data may be successfully explained by theories developed for x-ray absorption.[26,27] In a typical experimental setup, the double-differential cross section (6) may have contributions from matrix elements (11) with many different values of q. The requirement for the correct use of the dipole approximation may therefore be formulated as the condition that those matrix elements (11) which have a dominant contribution to an expression of the form (6) (which will be more complicated when allowance is made for any multiple scattering of the projectile electrons) satisfy a requirement of the form (37).

B. The effect of the excited state

The preceding argument is the simplest for estimating the value of q_d. The limitation of the argument is that it does not involve the properties of the state $R_{l'}(\epsilon,r)$ of the ejected electron, and cannot therefore address the question of any possible dependence of q_d on the energy ϵ of the ejected electron. It is this dependence which needs to

be examined in, for example, comparing the limits of the dipole approximation in the near-edge (ELNES) and extended fine-structure (EXELFS) regions. We can study this with the following treatment, in which we explicitly take account of the forms of the excited states $R_{l'}$, and compare the magnitudes of the first *two* leading terms in the expansion of (27) in a power series in q.

With the expansions (31)–(34) in (30) and (27) we find

$$\frac{\partial^2\sigma}{\partial E_f \partial\Omega}=\frac{1}{\pi^2}\frac{k_f}{k_i}k\left[\frac{1}{q^2}\pm\frac{1}{k_f^2}\right]^2\{q^2[\tfrac{1}{3}(I_1^1)^2]+q^4[\tfrac{1}{36}(I_2^0)^2+\tfrac{1}{15}(I_1^1 I_3^1)+\tfrac{1}{45}(I_2^2)^2]+O(q^6)\}\ , \tag{40}$$

where

$$I_p^{l'}=\int_0^\infty \phi_{10}(r)r^p R_{l'}(\epsilon,r)r^2 dr\ . \tag{41}$$

For the smallest values of q only the term in q^2 will be important. The superscript on the integral I for this term has the value $l'=1$ indicating the operation of the dipole selection rule (39) for sufficiently small q. As q is increased, however, it is clear that the term in q^4 will begin to make a significant contribution to (40). This term has contributions from excited states with $l'=0$ and 2 in addition to $l'=1$. What we do next depends on how we choose to define the dipole approximation. Strictly speaking, a matrix elements of the form (11) reduces to one of electric-dipole form only when the term linear in **q** dominates all the others. this linear term contributes only to the term quadratic in q in (40). However, in determining whether EXAFS or XANES theories well approximate EXELFS and ELNES, it is probably more important to examine the conditions under which the contributions of the $l'=1$ states dominate over all others (for the excitation of core states with $l=0$) because diffraction effects arising from the backscattering of the ejected atomic electrons are generally much stronger determinants of the energy-dependent fine structure than the weaker dependence of the matrix elements on energy. This defines the "dipole" limit as the one in which the electric-dipole selection rule (39) applies, rather than the one in which the EELS matrix elements reduce to precisely those of electric-dipole form. It is this definition that we adopt in this paper. The presence of $l'=1$ contributions to the quartic term in (40) shows the two definitions to be not quite equivalent. We mention in passing that our definition was implicitly used by De Crescenzi *et al.*[14] in their numerical comparisons of the contributions of the different values of l'.

Grouping together contributions to $l'=1$ on the one hand and those to $l'=0$ and 2 on the other, we see that the dipole selection rule may be safely assumed if

$$q^2[\tfrac{1}{3}(I_1^1)^2]+q^4[\tfrac{1}{15}(I_1^1 I_3^1)]\gg q^4[\tfrac{1}{36}(I_2^0)^2+\tfrac{1}{45}(I_2^2)^2]\ , \tag{42}$$

which leads to the condition that

$$q\ll q_d\ , \tag{43}$$

where

$$q_d=\frac{I_1^1}{[\tfrac{1}{12}(I_2^0)^2+\tfrac{1}{15}(I_2^2)^2-\tfrac{1}{5}(I_1^1 I_3^1)]^{1/2}}\ . \tag{44}$$

In the next section we show how this expression may be conveniently evaluated on a hydrogenic model, which may be expected to be particularly accurate for the excitation of K-shell electrons, to yield an analytic expression for $q_{\max}$ as a function of the atomic number Z of the atom being excited and of the energy ϵ of the excited electrons.

IV. THE HYDROGENIC MODEL

Since the early days of quantum mechanics, it was realized that reasonable analytic approximations to atomic wave functions may be obtained by assuming that the electrons of a particular shell move under the influence of a central potential of the Coulombic form

$$V(r)=-\frac{Z^*}{r}\ , \tag{45}$$

where Z^* is an effective nuclear charge, given by

$$Z^*=Z-s\ , \tag{46}$$

where s is known as a shielding constant, whose magnitude depends on the electron shell being considered. The justification for this approximation is that the charge density for electrons of a particular shell tends to be concentrated over quite a small range of distances from the nucleus, and so the magnitude of the shielding of the nuclear charge due to all the other electrons may be found quite accurately. For K shell, Slater[28] has estimated that $s=0.3$. This is the model we employ in the following. It is sometime known as the hydrogenic model, although, of course, it is applicable to the K shells of all elements.

On this model K shell wave functions are represented by

$$\phi_{10}(r)=2Z^{*3/2}e^{-Z^* r}\ . \tag{47}$$

For the potential (45), analytic expressions exist also for the radial wave functions $R_l(\epsilon,r)$ of positive energy ϵ, namely the Coulomb wave functions:[29]

$$R_l(\epsilon,r)=\frac{1}{(2l+1)!}\exp\left[\frac{\pi Z^*}{2k}\right](2kr)^l\left|\Gamma\left[l+1-\frac{iZ^*}{k}\right]\right|e^{-ikr}{}_1F_1\left[l+1+\frac{iZ^*}{k},2l+2,2ikr\right] \quad (48)$$

expressed in terms of $k(=\sqrt{2\epsilon})$, the wave vector of the ejected atomic electron of energy ϵ. Also in the above expression Γ and ${}_1F_1$ are the Gamma and confluent hypergeometric functions, respectively. The Coulomb wave function (48) manifests the asymptotic behavior at large r:

$$R_l\sim\frac{1}{kr}\sin\left[kr+\frac{1}{k}\ln(2kr)-\tfrac{1}{2}l\pi+d_l\right], \quad (49)$$

where

$$d_l=\arg\left[\Gamma\left[l+1-\frac{iZ^*}{k}\right]\right]. \quad (50)$$

Our aim is to evaluate the radial matrix elements (41). The justification for the use of the preceding approximations to the atomic radial wave functions is illustrated in Fig. 1. Here the analytic core and excited-state wave functions are compared, for the case of Ni ($Z=28$), an element which lies approximately in the middle of our range of interest, with radial wave functions calculated in the now conventional manner, by outward integration of the radial Schrödinger equation, for an atomic muffin-tin potential, constructed by the Mattheiss prescription,[30,31] starting with Herman-Skillman atomic wave functions.[32] The analytic $1s$ bound-state wave function agrees very

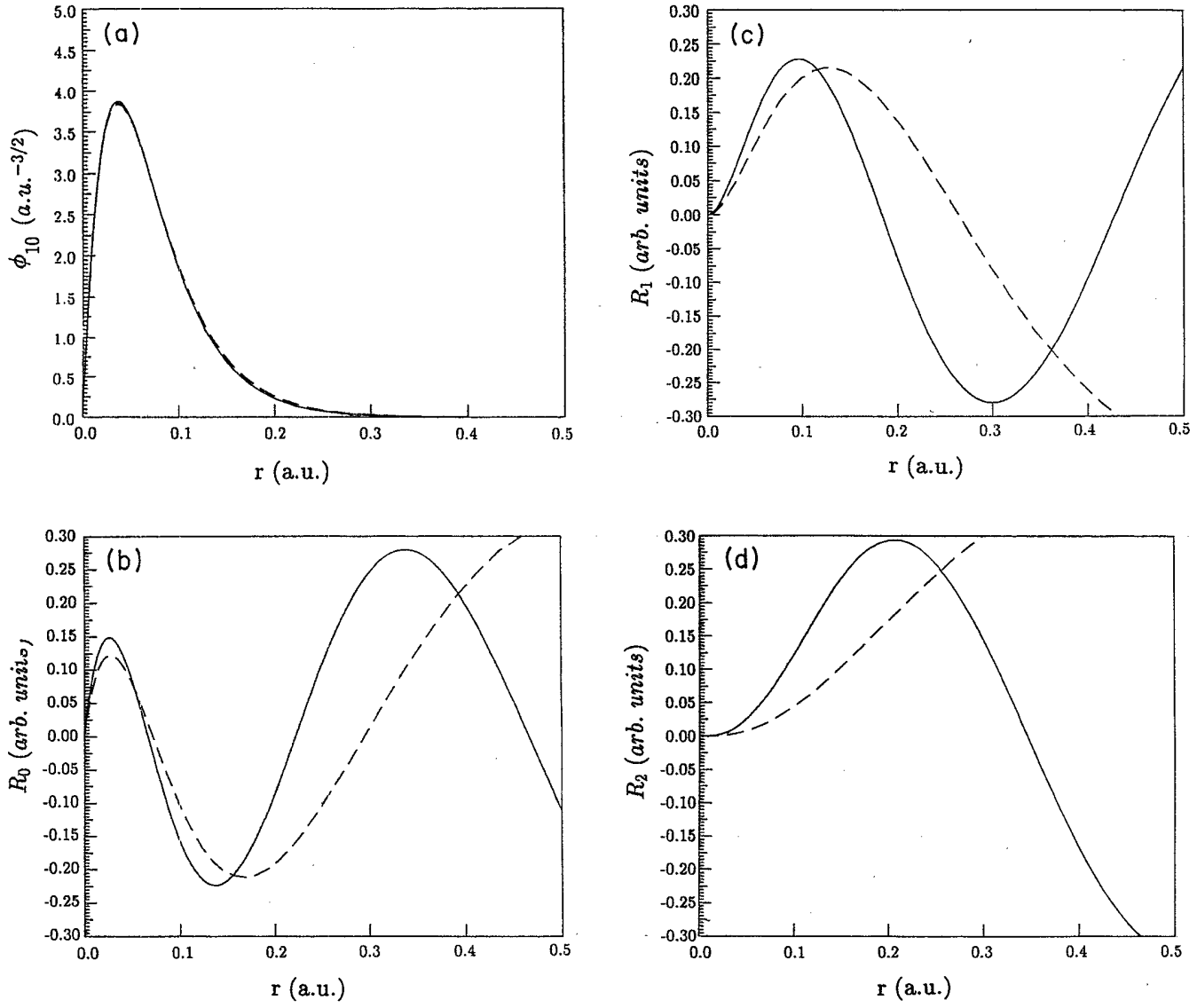

FIG. 1. Comparison of analytic and computed wave functions for Ni ($Z=28$). (a) $1s$ core wave function. Excited state wave functions $R_{l'}$ for $k=1$ (a.u.)$^{-1}$ ($\epsilon=0.5$ Hartree$\simeq$13.6 eV) and (b) $l'=0$, (c) $l'=1$, and (d) $l'=2$.

well with its numerical counterpart. Note that it occupies a radial extent of not much more than $\simeq 0.1$ a.u. Due to the form of the integrand in the radial matrix element, it is apparent that the only part of the excited-state wave function which contributes significantly to the matrix element is that which overlaps with the core wave function. In this region, the shielding parameter, s, for the excited-state wave function would be expected to be the same as that for the core wave function, and this justifies the use of the same effective nuclear charge, Z^* in (48). Although, as might be expected, the numerical and analytic excited-state wave functions differ substantially at large radii, their agreement in their region of common overlap with the core wave function is seen to be good. The greatest difference is observed for the $l'=2$ wave function, but this contributes only to the I_2^2 term in (44), which is small compared with the other two in the denominator, and would not be expected to significantly alter the value of q_d, our main quantity of interest. The result that the matrix elements involving coupling to the $l'=0$ states are generally much larger than those to the $l'=2$ states for K-shell excitations, has also been noted by others.[12,15]

With these analytic radial wave functions, we may use the result:[33]

$$\int_0^\infty e^{-st}t^{b-1}{}_1F_1(a,c,k't)dt=\Gamma(b)s^{-b}F(a,b,c,k's^{-1}) \tag{51}$$

provided

$$|k's^{-1}|<1\ , \tag{52}$$

where F represents the hypergeometric function,[34] to express the radial integrals in the closed form:

$$I_p^{l'}=2Z^{*3/2}\frac{1}{(2l'+1)!}\exp\left[\frac{\pi Z^*}{2k}\right](2k)^{l'}\Gamma\left[l'+1-i\frac{Z^*}{k}\right]\Gamma(l'+1+3)(Z^*+ik)^{(l'+p+3)}$$
$$\times F\left[l'+1+i\frac{Z^*}{k},l'+p+3,2l'+2,\frac{2ik}{Z^*+ik}\right]\ . \tag{53}$$

Using (48) in (41) we find

$$q_d=k\frac{A}{\sqrt{B}}\ , \tag{54}$$

where

$$A=|1-i\alpha|F(2+i\alpha,5,4;z) \tag{55}$$

$$B=\tfrac{3}{4}[F(1+i\alpha,5,4;z)]^2-6\exp(2i\tan^{-1}\alpha)F(2+i\alpha,5,4;z)F(2+i\alpha,7,4;z)$$
$$+\frac{3}{5}\frac{|2-i\alpha|^2}{(1-i\alpha)^2}\exp(2i\tan^{-1}\alpha)[F(3+i\alpha,7,6;z)]^2 \tag{56}$$

and

$$\alpha=\frac{Z^*}{k}\ , \tag{57}$$

$$z=\frac{2}{1-i\alpha}\ . \tag{58}$$

The hypergeometric functions F, may be evaluated from the power series:[34]

$$F(a,b,c;z)=1+\frac{ab}{1!c}z+\frac{a(a+1)b(b+1)}{2!c(c+1)}z^2$$
$$+\frac{a(a+1)\cdots(a+n-1)b(b+1)\cdots(b+n-1)}{n!c(c+1)\cdots(c+n-1)}z^n+\cdots\ , \tag{59}$$

which is convergent if $|z|<1$. This is equivalent to the condition (52) and they both require that

$$k<\frac{Z^*}{\sqrt{3}}\ . \tag{60}$$

V. RESULTS

The preceding analysis shows that, at least within the limits set by (60), which are not very stringent for most elements, q_d is a function of just two variables, namely

the effective nuclear charge Z^* and the wavevector k, of the ejected core electrons. To illustrate the behavior of this function, we plot, in Fig. 2, q_d against Z^* for Z^* ranging from about 2 to 50 and $k=1$. Bearing in mind the relationship

$$\epsilon=\tfrac{1}{2}k^2 \tag{61}$$

in atomic units, this corresponds to an energy of $\frac{1}{2}$ Hartree or 13.6 eV, which lies in the ELNES range of energies. Note that, since for K shells, the shielding charge s is very small, $Z^*\simeq Z$. Since our theory is nonrelativistic, we have restricted ourselves to a range of chemical elements with Z up to about 50. In Fig. 2, a nearly straight line of unit gradient is obtained, with barely perceptible deviations in the low Z^* limit.

In Fig. 3 we plot q_d against ϵ for specific values of Z covering the range up to $Z=50$. In all cases, q_d reduces a little from its low-ϵ limit of Z^* as the energy is increased into the EXELFS's range of energies.

We can gain further insight into these results by noting that q_d/k is a function of the single parameter $\alpha(=Z^*/k)$. Given the fact that, in Fig. 2, we have plotted q_d versus Z^* for $k=1$, that Figure can also be regarded as a plot of q_d/k against α, with the same numerical values on the two axes. In the high-α limit (low k), clearly

$$\frac{q_d}{k}\simeq\frac{Z^*}{k} \tag{62}$$

and hence

$$q_d=Z^*(\simeq Z)\,, \tag{63}$$

as is indicated by Fig. 2. For low α, on the other hand, (i.e., high k or ϵ) we see also from the reinterpreted Fig. 2, that

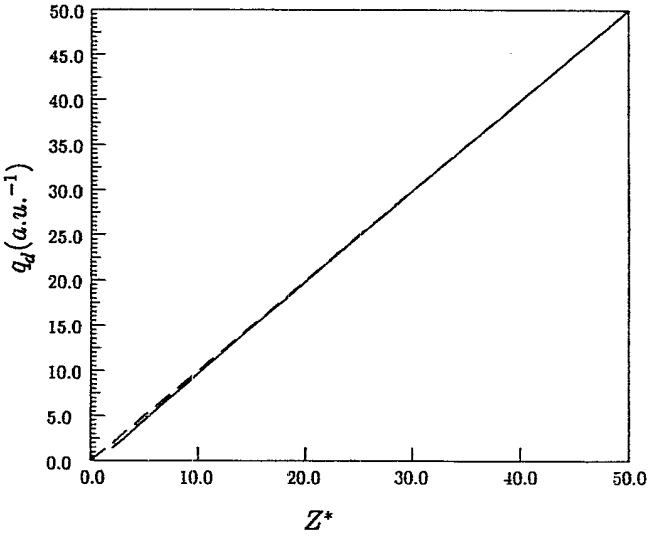

FIG. 2. Plot of q_d vs the effective nuclear charge Z^* for $\epsilon=13.6$ eV $[k=1(\text{a.u.})^{-1}]$.

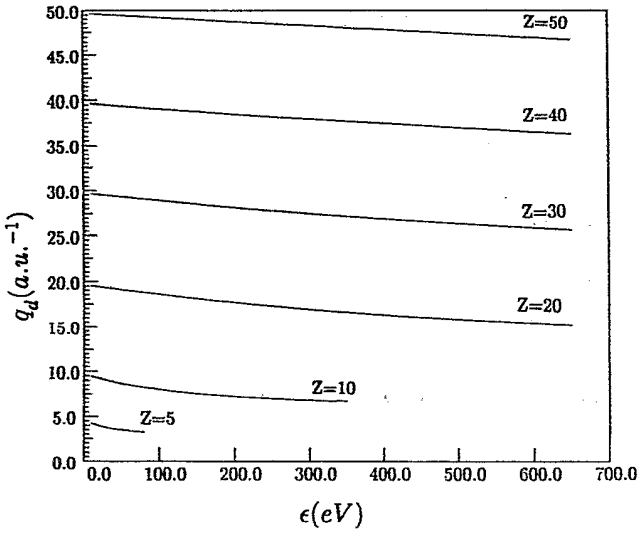

FIG. 3. Plot of q_d vs the energy of the ejected core electron ϵ for selected values of the atomic number Z.

$$\frac{q_d}{k}<\alpha\left[=\frac{Z^*}{k}\right] \tag{64}$$

and therefore

$$q_d<Z^*(\simeq Z)\,. \tag{65}$$

Thus we see that the interpretation of Fig. 2 as a plot of q_d/k against α leads to an understanding of both of the original Figs. 2 and 3. Nevertheless, we retain the original forms of Figs. 2 and 3 as they are probably the most pertinent from the point of view of an experimentalist.

As for the restriction implied by (60), this is equivalent to the condition that

$$\epsilon<\epsilon_{\max}\,, \tag{66}$$

$$\epsilon_{\max}=\frac{Z^{*2}}{6}\,. \tag{67}$$

The values of $\epsilon_{\max}$ for a few selected elements are given in Table I. It is clear that for even the first solid element (Li,$Z=3$) our analysis is valid over essentially all of the XANES range of energies, and that for elements as light as O ($Z=8$) it covers the energy range over 250 eV from the absorption edge, adequate for an EXAFS analysis.[26,35]

TABLE I. Values of $\epsilon_{\max}$ for various elements.

Element	Z	Hartrees	eV
H	1	0.16	4.5
He	2	0.48	13
Li	3	1.22	33
Be	4	2.28	62
O	8	9.88	269
F	9	12.6	343
Ag	47	363	9879

VI. DISCUSSION

If an electron-energy-loss experiment were being performed on an isolated atom, with well-defined directions of the incident and detected electrons, and if the magnitude of the energy loss were known, $\mathbf{q}$ could be determined precisely by (12). On the other hand, when an EELS experiment is performed on a sample of condensed matter, even if these experimental conditions were well known, the coexistence of many elastic-scattering paths in the material, results in a wide range of momentum-transfer vectors $\mathbf{q}$ in the many inelastic-scattering processes contributing to the measured signal. In a crystalline sample this may be quantified to some extent,[15–20] but in general we gain much understanding by considering the range of possible values of q. Its minimum value

$$q_{\min}=k_i-k_f \tag{68}$$

corresponds to inelastic forward scattering, and is an inevitable consequence of the fact that, by definition, the incident electron loses energy. In general q may be greater than $q_{\min}$ because, in addition, the electron can change direction. The theoretical maximum value of q is

$$q_{\max}=k_i+k_f \tag{69}$$

when the incident electron is inelastically back scattered. Many authors[36–39] have preferred to assume a more restrictive value of $q_{\max}$ corresponding to the Bethe ridge[14,40] of enhanced magnitude of the generalized oscillator strength,[13] namely

$$q_{\max}=(k_i^2-k_f^2)^{1/2} \tag{70}$$

when the relationship between $\mathbf{k}_i$, $\mathbf{k}_f$, and $\mathbf{q}_{\max}$ may be given the graphical representation of the three sides of a right-angled triangle, where $\mathbf{k}_i$ forms the hypoteneuse.

Regardless of the magnitude assumed for $q_{\max}$, the existence of a negative power of q in expressions (e.g., 25) for the measured signal implies that, in general, the lowest values of q, namely those around $q_{\min}$, tend to dominate the signal. As a result, the precise value taken for $q_{\max}$ is of little consequence. Given that, from Sec. V, the dipole approximation breaks down when q becomes comparable with q_d, a necessary condition for the dipole approximation in a sample of condensed matter must be

$$q_{\min}\ll q_d \ . \tag{71}$$

From (68) it follows that

$$q_{\min}=\sqrt{2E_i}-\sqrt{2E_f} \ , \tag{72}$$

where

$$E_f=E_i-\Delta E \tag{73}$$

and

$$\Delta E=E_K+\epsilon \ , \tag{74}$$

where E_K is the ionization energy of the core electron. Thus we may write

$$q_{\min}=\sqrt{2E_i}[1-(1-\Delta E/E_i)^{1/2}] \ . \tag{75}$$

Noting that the requirement that $E_f\geq 0$ implies that ϵ can range from zero up to E_i-E_K, the dashed lines in Fig. 4 show the variation of $q_{\min}$ against ϵ for several different incident electron energies E_i for the excitation of the Si K edge, where $E_K=1839$ eV.[41] Where possible, the value of ϵ is allowed to vary from zero to about 650 eV to cover the near edge as well as EXELFS ranges. At the threshold for the excitation of a K edge, $E_i=E_K$ and the extent of the dashed lines shrinks to a single point. At this threshold $q_{\min}$ takes the value

$$q_{\min}=\sqrt{2E_K} \tag{76}$$

marked by the cross on Fig. 4.

Similar curves have been plotted by Nassiopoulos and Cazaux,[38,39] who have noted the decrease in $q_{\min}$ with increasing E_i for a given ΔE (or ϵ) and the increase in $q_{\min}$ with ΔE for a given E_i. However, in order to draw any conclusions regarding the relative ease of satisfying the condition (71) for the dipole approximation in the different regions of an energy loss spectrum, it is necessary to compare $q_{\min}$ and q_d as functions of ϵ. Due to the lack of an expression for the explicit dependence of q_d on ϵ, this has not been possible to date. Using our expressions (54–59) we are able to examine this question by plotting on the same Fig. 4 for a particular element (Si) the variation of q_d with ϵ.

The graphical implication of condition (71) is that the curves representing $q_{\min}$ should lie substantially lower than that representing q_d. Due to the fact that $q_{\min}$ increases with ϵ for any given value of E_i and that q_d decreases with the same quantity it is clear from Fig. 4 that it is generally significantly easier to satisfy the conditions

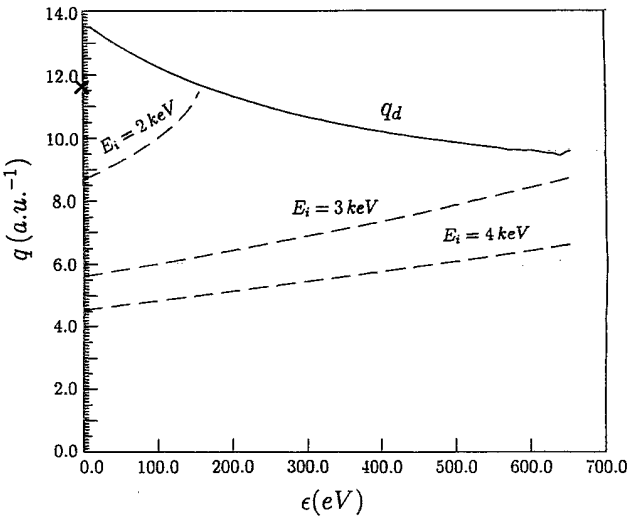

FIG. 4. Comparison of q_d (solid line) and $q_{\min}$ (dashed lines) for the Si K edge as a function of ϵ. The different dashed lines indicate the dependence of $q_{\min}$ on the energy, E_i, of the incident electrons. The cross marks the limiting value of $q_{\min}$ at the ionization threshold, when $E_i=E_K(=1839$ eV).

for the dipole approximation in the near-edge region (small ϵ) than that of the extended fine structures (large ϵ).

We have used the angular-momentum representation of unbound Coulombic wave functions for the states of the ejected atomic elements, unlike some other authors,[16,42] who used the form which has the far-field asymptotic limit of a plane wave. Such a (linear momentum) representation may be the most appropriate if the ejected atomic electron is detected in the far field by a small-angle detector [i.e., in a so-called $(e,2e)$ experiment]. Such experiments are difficult, at least in the solid state, since they require the two final-state electrons to be detected in coincidence. On the other hand, in a conventional EELS experiment, as has been pointed out by Saldin and Rez,[17] the ejected atomic electron is not detected directly—only its effect on the energy-loss cross section of the incident electron (assuming negligible exchange effects). If the linear-momentum-resolved Coulombic wave functions are used for the ejected electrons, it is necessary to perform an additional angular integration over all directions of emission of these electrons,[16] in order to recover the double-differential cross section (6). The need for this second integral is eliminated by our use of the angular-momentum representation. Also, of course, this is the most appropriate representation for quantifying the effects of the angular momentum selection rules, which we do in our investigation of the dipole approximation.

VII. CONCLUSIONS

We have examined the upper limit q_d of the magnitude of the momentum-transfer vector $\mathbf{q}$ for the justifiable assumption of the dipole approximation in K-shell electron-energy-loss spectroscopy. Using atomic wave functions based on a hydrogenic model, we find, for the first time, an analytic expression for q_d, as a function of both atomic number, Z, and energy ϵ of the ejected core electron. We find that q_d only asymptotically approaches the value, Z^*, assumed by current theory in the limit of small ϵ, and that it falls noticeably below this value for larger ϵ.

The existence of many elastic scattering paths in a typical EELS experiment results in inelastic scattering events characterized by many different values of q, but those which dominate the measured signal are ones for which $q \simeq q_{\min}$, the minimum possible value. The increase of $q_{\min}$ with ϵ coupled with a corresponding decrease of q_d indicates a greater ease of satisfying the conditions for the dipole approximation in the near edge, rather than extended fine-structure regions of the spectra. Our analytic approach is well suited for generalization to other atomic core edges (e.g., L, M, edges, etc.)

[1]R. F. Egerton, *Electron Energy Loss Spectroscopy in the Electron Microscope* (Plenum, New York, 1986).
[2]M. Siegbahn, Philos. Mag. **37**, 601 (1919).
[3]E. A. Stern, Phys. Rev. B **10**, 3027 (1974).
[4]J. J. Ritsko, S. E. Schnatterly, and P. C. Gibbons, Phys. Rev. Lett. **32**, 671 (1974).
[5]P. J. Durham, J. B. Pendry, and C. H. Hodges, Comput. Phys. Commun. **29**, 193 (1982).
[6]J. Taftø and J. Zhu, Ultramicroscopy **9**, 349 (1982).
[7]P. A. Lee and J. B. Pendry, Phys. Rev. B **11**, 2795 (1975).
[8]C. A. Ashley and S. Doniach, Phys. Rev. B **11**, 1279 (1975).
[9]R. D. Leapman and V. E. Cosslett, J. Phys. D **9**, L29 (1976).
[10]L. A. Grunes and R. D. Leapman, Phys. Rev. B **22**, 3778 (1980).
[11]J. Auerhammer and P. Rez, Phys. Rev. B **40**, 2024 (1989).
[12]P. Rez, Ultramicroscopy **28**, 16 (1989).
[13]H. A. Bethe, Ann. Phys. (N.Y.) **5**, 325 (1930).
[14]R. F. Egerton, Ultramicroscopy **4**, 169 (1979).
[15]M. De Crescenzi, L. Lozzi, P. Picozzi, S. Santucci, M. Benfatto, and C. R. Natoli, Phys. Rev. B **39**, 8409 (1989).
[16]C. J. Rossouw and V. M. Maslen, Philos. Mag. **A49**, 743 (1984).
[17]D. K. Saldin and P. Rez, Philos. Mag. **B55**, 481 (1987).
[18]D. K. Saldin, Philos Mag. **B56**, 515 (1987).
[19]F. Mila and C. Noguera, J. Phys. C **20**, 3863 (1987).
[20]D. K. Saldin, Phys. Rev. Lett. **60**, 1197 (1988).
[21]D. J. H. Cockayne, I. L. F. Ray, and M. J. Whelan, Philos. Mag. **20**, 1265 (1969).
[22]J. B. Pendry and D. K. Saldin, Surf. Sci. **145**, 33 (1984).
[23]V. I. Ochkur, Zh. Eksp. Teor. Fiz. **47**, 1746 (1964) [Sov. Phys.—JETP **20**, 1175 (1965)].
[24]J. S. Faulkner and G. M. Stocks, Phys. Rev. B **21**, 3222 (1980).
[25]A. Messiah, *Quantum Mechanics* (Wiley, New York, 1966), Vol. II, p. 1054.
[26]M. De Crescenzi, F. Antonageli, C. Bellini, and R. Rosei, Phys. Rev. Lett. **50**, 1949 (1983).
[27]M. M. Disko, J. C. H. Spence, O. F. Sankey, and D. Saldin, Phys. Rev. B **33**, 5642 (1986).
[28]J. C. Slater, Phys. Rev. **36**, 57 (1930).
[29]L. D. Landau and E. M. Lifshitz, *Quantum Mechanics* (Pergamon, Oxford, 1977), p. 121.
[30]L. F. Mattheiss, Phys. Rev. A **133**, 1399 (1964).
[31]T. L. Loucks, *The Augmented Plane Wave Method* (Benjamin, New York, 1967).
[32]F. Herman and S. Skillman, *Atomic Structure Calculations* (Prentice-Hall, Englewood Cliffs, 1963).
[33]I. S. Gradshteyn and I. M. Ryzhik, *Table of Integrals, Series and Products* (Academic, New York, 1965).
[34]M. Abramowitz and I. A. Stegun, *Handbook of Mathematical Functions* (Dover, New York, 1972).
[35]J. Stöhr, R. Jaeger, J. Feldhaus, S. Brennan, D. Norman, and G. Apai, Appl. Opt. **19**, 3911 (1980).
[36]M. Inokuti, Rev. Mod. Phys. **43**, 297 (1971).
[37]C. J. Powell, Surf. Sci. **44**, 29 (1974).
[38]A. G. Nassiopoulos and J. Cazaux, Surf. Sci. **149**, 313 (1985).
[39]A. G. Nassiopoulos and J. Cazaux, Surf. Sci. **165**, 203 (1986).
[40]H. A. Bethe and R. W. Jackiw, *Intermediate Quantum Mechanics* (Benjamin, New York, 1968).
[41]C. C. Ahn and O. L. Krivanek *EELS Atlas* (Arizona State University, Tempe, 1983).
[42]L. J. Allen and C. J. Rossouw, Phys. Rev. B **38**, 2232 (1988).